SINTERING RESPONSE AND MECHANICAL PROPERTIES OF MICROWAVE SINTERED 316L POWDER BLENDS

João Mascarenhas, Teresa Marcelo
INETI, Department of Materials and Production Technologies
Azinhaga dos Lameiros, 1649-038 Lisbon, Portugal; joao.mascarenhas@ineti.pt

Abstract Microwave sintering can be an efficient, economic and valuable approach for the processing of some PM materials. Recent findings on the ability of powdered metals to absorb and dissipate microwave radiation, opened new opportunities for the PM world. Being the particle size of the metallic powders one of the key parameters that rules the heating rate and the temperature performance during microwave sintering, work has been carried out on compacts of 316L powder blends with 60, 50, 25 and 7 μm mean particle sizes, at 1150ºC for 30 minutes in a 2.45 GHz-1000 W microwave oven. Green and sintered densities and corresponding transverse rupture strength (TRS) are reported as well as hardness and porosity. Densities in excess of 95% were attained for the finer powders. TRS tests were performed on all but the 7 μm powder specimens, being the highest value of 630 MPa obtained for the 25 μm powder specimens.

Introduction

Energy is a today's major concern and on the industrial point of view, this is a double concern, one being the production costs related with processes' energy efficiency, along with the environmental approach. Traditional sintering of stainless steels is carried out in conventional electric sintering furnaces, using slow heating rates in order to prevent thermal gradients in the powder compacts [1]. Regarding these subjects, microwave (MW) sintering can be an important approach, as it can reduce both sintering times and temperatures along with faster heating rates and homogeneous specimens heating, these being in addition to all the already known PM advantages. In fact, savings of 90% in sintering cycles were already reported [2] when MW is compared to conventional vacuum sintering.

In the last years, several studies have shown that microwave sintering of particulate materials is possible [3]. Though these studies being more copious for dielectric materials, like ceramics, some authors have shown that it is also viable for metal powders [3] and more particularly for stainless steels powder compacts [2,4,5]. Modelling of microwave sintering of particulate metals has stated that it is influenced by several material characteristics, one of them being particle size [3,6]. This influence is closely related to the depth of MW penetration in materials, a parameter known as skin depth δ in the case of conductive materials [3] and given by:

$$\delta = \frac{1}{\sqrt{\pi f \mu \sigma}} = \sqrt{\frac{\rho \lambda_0}{\pi c \mu}} \qquad (1)$$

where f is the microwave frequency, σ is the electrical conductivity, μ is the magnetic permeability in free space ($4\pi x10^{-7}$ $H.m^{-1}$), ρ is the electrical resistivity, λ_0 is the microwave wavelength and c is the speed of light. As λ_0 is a constant for each MW frequency (12.24 cm for 2.45 GHz), δ becomes dependent only on the electrical resistivity ρ.

For most of the metals, δ is within the range 0.1 - 10 μm [5]. Thus, for a specific powdered metal, if δ is comparable to the mean particle size, energy dissipation of the incident radiation will be more efficient thus favouring heat transfer and finally sintering.

The present work is part of a research centred on PM 316L stainless steel and dealing with several material parameters influence on different sintering approaches. Particle size effect on the solid state MW sintering of 316L compacts is studied.

EXPERIMENTAL

Gas atomized (GA) and water atomized (WA) 316L powders were blended with GA to WA ratios of 50:50 and 20:80, the mean particle sizes (d_{50}) of the blends as well as those of the starting powders being measured by laser diffraction. The four powders were uniaxially

compressed into 20 mm diameter, 3-4 mm high cylinders, the compacting pressure varying between 465 and 1240 MPa, and also into rectangular cross section TRS (transverse rupture strength) specimens of 31.8 x 12.7 x 7 mm^3 at 730 MPa.
Sintering was carried out in a 2.45 GHz–1000 W microwave furnace. A type S thermocouple shielded with Pt foil, connected to a controller, was used just above the sample to control the sintering temperature. A ceramic thermal pod and SiC susceptor blocks to assist heating up from room temperature were used as shown in Figure 1; the experiments were carried out under flowing argon (inside and outside the pod). The cylinders were sintered at 1150ºC (solid state sintering) for 10 and 30 minutes, heating up either freely to the sintering temperature or following a controlled rate (40ºC/min) using the signal from the thermocouple to automatically switch on/off the power, according to the programmed heating rate.
The rectangular specimens were microwave sintered at 1150ºC - 30 minutes - 40ºC/min of programmed heating rate and then bend tested in a 3 point jig to evaluate the TRS according to ISO 3325 standard. Green strength was also evaluated on the rectangular specimens of the same powders according to ISO 3995 standard. TRS tests were not performed on the GA powder.

Figure 1 – Experimental arrangement used for MW sintering.

Geometrical density was evaluated on the as-pressed and the as-sintered materials; density was also evaluated by water pycnometry on some selected sintered cylinders. Samples were taken from the sintered cylinders for X-ray Diffraction (XRD, CuK_α radiation) and for O_2 (IR absorption) and N_2 (thermal conductivity) analysis; these analyses were also carried out on the starting powders for comparison purposes.
Microstructural characterisation was carried out on mounted and polished longitudinal cross sections taken from the sintered cylinders; it included Optical and Scanning Electron Microscopy with microanalysis by Energy Dispersive Spectrometry (OM, SEM/EDS).
Porosity quantification through Image Analysis of some optical micrographs was also carried out using the Axiovision Multiphase software. SEM was also used to observe the morphology of the starting powders as well as the fracture surfaces of the TRS specimens.
Microhardness Vickers HV was measured on some of the polished sections (10 indentations on each sample) using 25 g load on the sintered GA powder samples and 50 g load on the remaining ones.

Results and Discussion
The characterisation data of the 316L starting powders are summarized in Table 1 and the morphology of the loose powders as well as the microstructure of the particles cross sections are shown in Figure 2. The finest particle dimension is exhibited by the GA powder, hereafter referred to as 100F; accordingly, WA powder is identified as 0F (no fine GA particles added) and the blends as 20F and 50F. These blends have d_{50} of 50 and 25 μm, respectively.

Table 1 – Characteristics of the 316L starting powders.

316L powder	O_2 (wt. %)	N_2 (wt. %)	Phases detected (XRD)	d_{50} (μm)	Compressibility at 1240 MPa
WA (0F)	0.31	0.035	austenite	60 (90 v%<110 μm)	91%d_T
GA (100F)	0.14	0.123	austenite + ferrite	7 (90 v%< 18 μm)	87%d_T

Powders compressibility was evaluated through the green density of cylinders compacted at different pressures; the densities achieved at 1240 MPa are shown on Table 1 as a % of the theoretical density d_T of the PM 316L stainless steel (7.88 $g.cm^{-3}$). Green densities similar to that of the 0F powder were measured in the 20F and 100F blends compacted at the same pressure of 1240 MPa. The less ability of the 100F powder to be uniaxially compacted resulted in flake cracking of the compacted cylinders and precluded the manufacturing of sound rectangular cross section specimens for TRS evaluation.

WA

GA

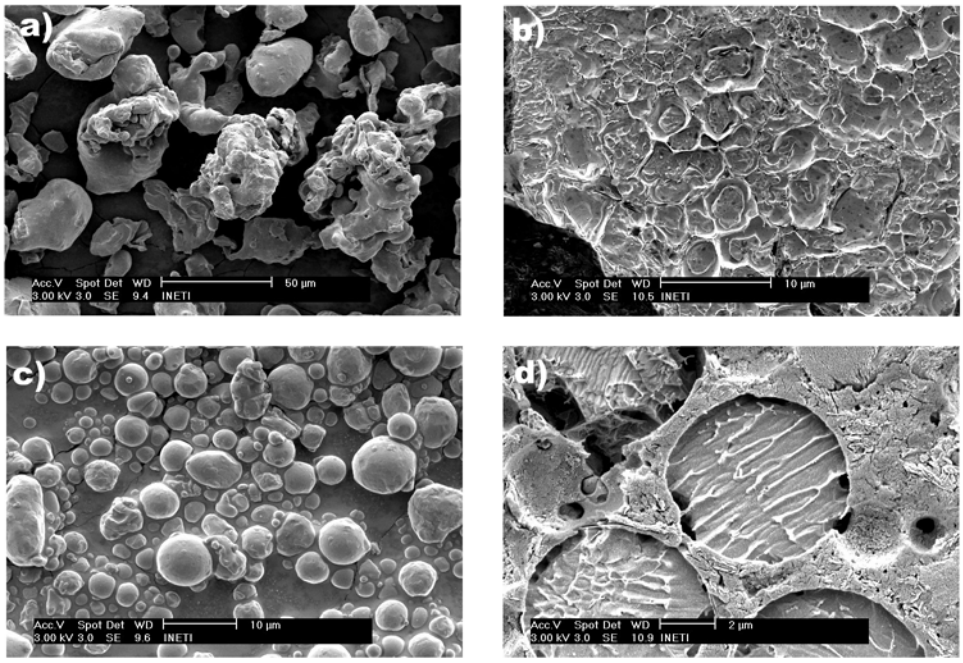

Figure 2 – SEM characterisation of the 316L starting powders: a) and c) loose powders morphology; b) and d) particles microstructure (polished cross sections).

MW sintering with non-programmed heating rate resulted in faster heating of the materials, 80-90ºC/min; a dramatic decrease of the heating rate above 800ºC was also found independently from the sintering cycle, the green density or the samples geometry. Although MW sintering has been carried out under flowing argon, some oxidation could not be avoided and an oxide layer formed on the surface of the samples, which partly affected the overall specimen density. However, the sintered specimens seem to have higher densification in the specimens' core, as was noted with the microstructural characterisation of polished sections.
Microstructural features (OM) of the MW sintered materials are shown in Figure 3. The highest densification was achieved for the 100F powder (d_{50} = 7 μm) sintered at the fastest heating rate (fig. 3-c); a volume fraction of 4.5% was measured (IA) for the porosity, the pores being mainly round shaped with equivalent circle diameters < 8 μm. Larger and angular shaped porosity can be seen in the materials containing the larger WA particles and sintered in the same conditions (figs. 3-a) and b); the volume fraction of porosity measured in these samples was 5.2% and 5.0% respectively for 0F and 50F and the corresponding equivalent circle diameters < 20 μm and < 8 μm. It is evident that there is a strong influence of the mean particle size on the degree of densification which can be related to the skin depth. Considering $740x10^{-9}$ Ω.m as the 316L electrical resistivity [7], δ = 8.7 μm was obtained using equation (1), a value slightly larger than d_{50} of the GA powder, thus it is possible that more than 50 weight % of the GA particles have been heated due solely to the MW energy dissipation.
Green density also seems to be an influencing parameter on the sintering response and the larger the mean particle size the higher the green density needed to have comparable densification after sintering, whichever the sintering cycle experimented. Observing Figs. 3-a), b) and c) it can be verified that when mean particle size is decreased, lower green densities are needed to achieve comparable densities upon sintering. In fact (though not

shown), when 0F, 20F and 50F specimens having green densities below 82%d_T were sintered, no densification occurred.
For a particular mean particle size and a green density high enough to promote densification, increasing the heating rate resulted in less porosity as is exemplified with the 100F material, comparing figures 3-c) (4.5% porosity) and f) (10% porosity), however, it should be noted that this behaviour is not so evident in the other blends due to the effect of larger particle size on densification.

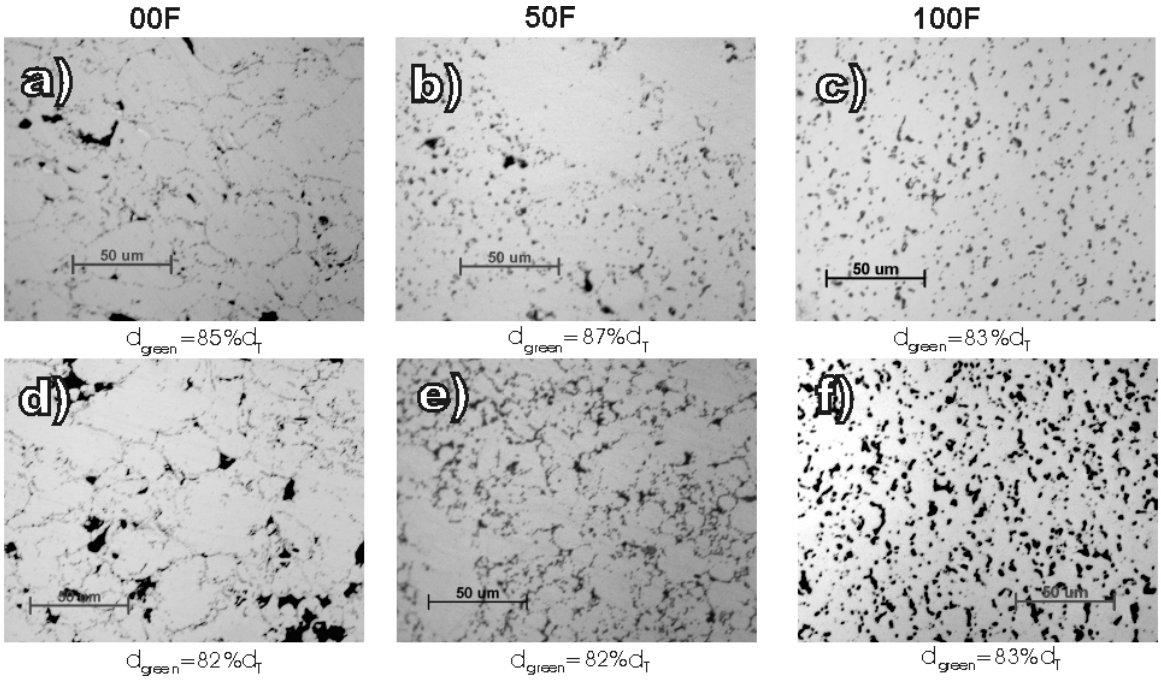

Figure 3 – Microstructural characterisation (OM) of 316L powder blends MW sintered at 1150ºC for: a) to c) 30 minutes - 80ºC/min; d) and e) 10 minutes - 40ºC/min; f) 30 minutes - 40ºC/min.

For the heating rate of 40ºC/min, it was found that after 10 minutes at 1150ºC, necking has already formed and some of the porosity is very fine and round as shown in Figures 4-a) and b); extending the sintering time up to 30 minutes did not improve the sintering response and the microstructures from 10 and 30 minutes are comparable. The grey phase pinning the powder particles in less dense areas, more evident in the materials containing the WA powder (figs. 3-a) and d) for example), is a Cr-rich oxide according to the OK_α and CrK_α X-ray line profiles obtained by SEM/EDS as illustrated in Figure 4-b). This is probably the Cr_2O_3 phase identified by XRD in some samples (PDF#38-1479 [8]).

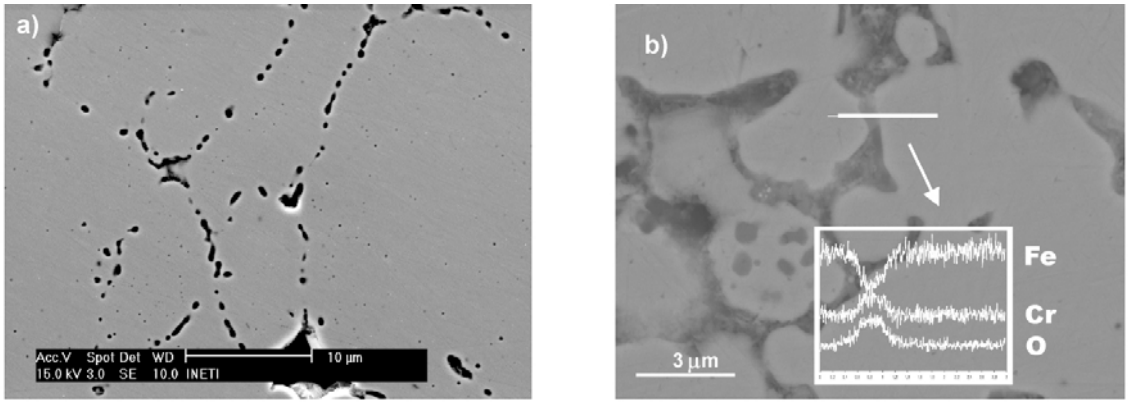

Figure 4 – SEM micrographs of 316L powders MW sintered at 1150ºC – 10 min. – 40ºC/min: a) 20F blend, secondary electrons image; b) 50F blend, OK_α, CrK_α and FeK_α XR line profiles on backscattered electrons image.

The oxide has contributed to the lower densification achieved by the WA powder based materials (0F, 20F) since it had an oxygen content as high as 0.3% (Table 1). In fact, observing the microstructures of the 100F materials (GA powder, O_2 = 0.14%), the particles are apparently strongly bonded and sintered and only at the prior particle interfaces some porosity and/or oxides are detected. However, all the sintered materials have high oxygen content, an average of 1.9 and 1.5wt% for 0F and 100F, respectively having been measured.
Figure 5 shows the XRD spectra obtained on the 0F and 100F materials MW sintered under the same conditions of 1150ºC – 30 min. – 80ºC/min. Besides the austenitic phase (PDF#31-619) and traces of Cr_2O_3 detected in the 0F sample, it can be seen that the Fe-Cr ferritic phase corresponding to the PDF#34-396 is also present, the amount being much larger in the 0F material than in the 100F one. However, as mentioned before and shown also on Fig. 5, ferrite was not present in the WA starting powder but indeed it is detected in most of the sintered materials; observation of etched surfaces (nital 2%, Vilella's reagent) was not conclusive on the ferritic phase distribution. Martensite was not detected by XRD and no other phases like carbides or Ni-rich phases were detected with the analytical resources available. It seems that there is some effect of the MW radiation on these ferrous alloys and further studies have to be carried on in order to understand the transformation mechanism possibly resulting from the interaction with the electromagnetic field.

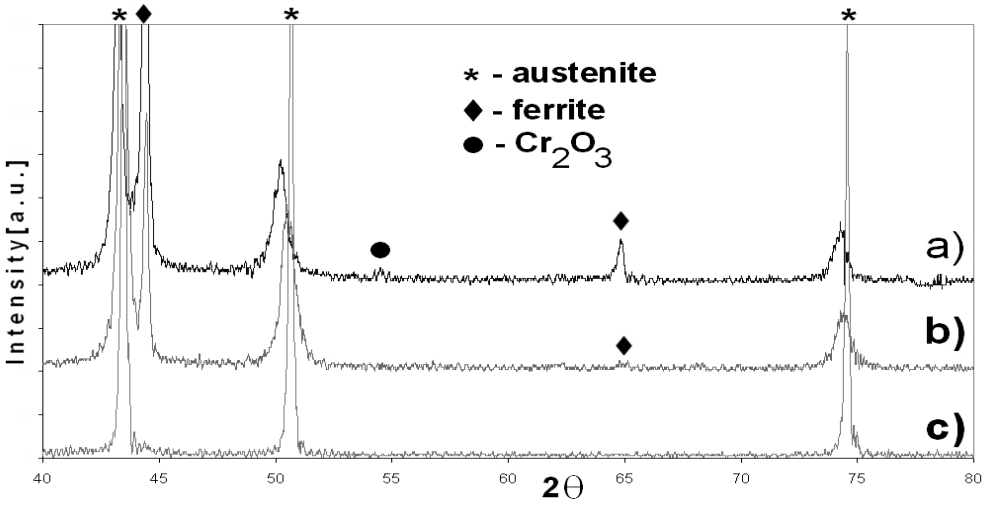

Figure 5 – XRD spectra of 316L powders: a) 0F and b) 100F, MW sintered at 1150ºC – 30 min – 80ºC/min; c) 0F(WA) powder, as-received.

The data obtained from the mechanical properties evaluated are shown in Table 2 (HV) and in Figures 6 (TRS) and 7 (fracture surfaces). As similar microhardness values were obtained within the specimens of the same powder blends, the results on Table 2 are the average values. This shows no influence of the experimental parameters on microhardness. The slightly higher value of HV = 250 obtained on the 0F material probably resulted from the larger amount of oxides, as shown before. On the other hand it seems microhardness was not affected by ferrite formation, this being possible if it is believed that the transformation has occurred mainly in the very fine particles, those with $d \leq \delta$ (not chosen for microhardness indentations) and more proun to be fully heated by the incident radiation.
Small addition of fine GA powder didn't have much influence on the sintered TRS, as shown on Fig. 6 and the less this amount was the lower the sintering degree achieved since the type of fracture observed (Fig. 7-a) is mainly inter-particle. The TRS of the 50F material is 160 MPa higher than the 0F and 20F ones and the dimples observed on the fracture surface (Fig. 7-b) are in accordance with that increment, this being an evidence that sintering was more effective. In fact, the fracture surfaces of 0F and 20F TRS specimens show powder particles that are not bonded, Fig. 7-a), this contributing to the lower TRS value, whilst 50F ones already show a more continuous bonding, Fig. 7-b) as confirmed by microstructural observations on Fig. 3. It is believed that due to the high oxide level of the WA powder (0F) sintering necks are not effective, being bonding performed amongst oxides. As one can

observe on Figs. 3-a) and d) a continuous oxide layer is present on the powder particle borders, contrarily to 100F specimens where sintering necks showed no chemical composition gradients, when compared to particles cores, as observed by X-ray line scans.

Table 2 – Vickers microhardness of 316L powders MW sintered at 1150ºC.

	0F	20F	50F	100F
HV	249 ± 12	224 ± 16	229 ± 19	230 ± 15

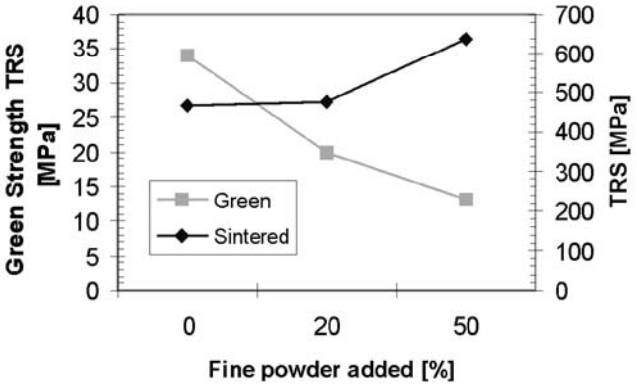

Figure 6 – Green and MW sintered TRS of 316L powder specimens.

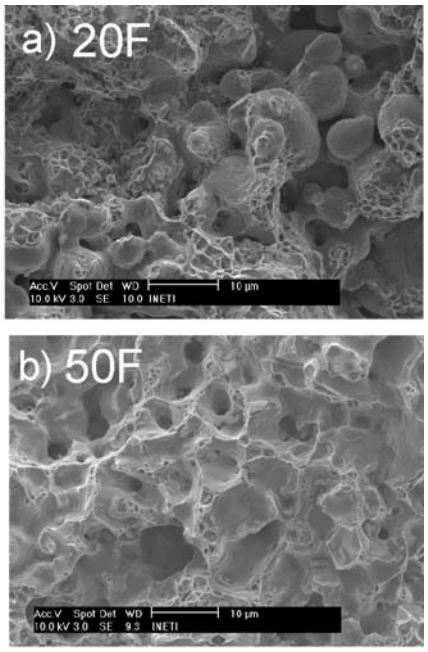

Figure 7 – Fracture surfaces (SEM) of 316L MW sintered TRS specimens.

Conclusions

Microwave solid state sintering is viable for 316L powders, being mean particle size and oxygen level two of the major factors to be controlled.

Though showing an acceptable porosity level (≈5%) for solid state sintering, 0F and 20F specimens had the lowest TRS values, this being attributed to the oxides on the particle surfaces, which did not allowed an effective sintering.

Effective sintering was attained in the 100F specimens, porosity being ≈4.5%, no precipitates being found on the sintering necks.

Acknowledgements

Thanks are due to Mr. Sérgio Tchikanha (FCUL) and to Dr. Filipe Neves (INETI); work was partly carried out at Materials Characterisation Laboratory (LCM/INETI).

References

[1] R. M. German, Sintering Theory and Practice, John Wiley, N.Y. USA, 1996.

[2] S.S. Panda, V. Sing, A. Upadhyaya, D. Agrawal, Sintering Response of Austenitic (316L) and Ferritic (434L) Stainless Steel Consolidated in Conventional and Microwave Furnaces, Scripta Materialia, 54, 2006, 2179 - 2183.

[3] K.J. Rao *et a*l., Rewiews: Synthesis of Inorganic Solids using Microwaves, Chem. Mater., 11, 1999, 882 – 895.

[4] P. Varonesi *et al*., Preliminary Studies of the Rapid Microwave Sintering of Green Parts Made of 420L Stainless Steel, Euro PM'2006, PIM, Poster show, Ghent, 2006.

[5] S.S. Panda, V. Sing, A. Upadhyaya, D. Agrawal, Effect of Conventional and Microwave Sintering on the Properties of Yttria Alumina Garnet-Dispersed Austenitic Stainless Steel, Metal. Mater. Trans. A, 37A, July 2006, 2253-2264.

[6] L.Z. Wu *et al*., Particle Size Influence to the Microwave Properties of Iron Based Magnetic Particulate Composites, Journal Magnetism Magnetic Materials, 285, 2006, 233-239.

[7] www.azom.com, 2007.

[8] ICDD, Powder Diffraction File-2, 2005, CD-ROM.